Electronic supplementary information (ESI) for

Hydrodeoxygenation of C4-C6 sugar alcohols to diols or mono-alcohols with retention of carbon chain over silica-supported tungsten oxide-modified platinum catalyst

Lujie Liu,[a] Ji Cao,[a] Yoshinao Nakagawa,[a,b,*] Mii Betchaku,[a] Masazumi Tamura,[c] Mizuho Yabushita,[a] and Keiichi Tomishige[a,b,*]

[a] *Department of Applied Chemistry, School of Engineering, Tohoku University, 6-6-07 Aoba, Aramaki, Aoba-ku, Sendai 980-8579, Japan*

[b] *Research Center for Rare Metal and Green Innovation, Tohoku University, 468-1 Aoba, Aramaki, Aoba-ku, Sendai 980-0845, Japan*

[c] *Research Center for Artificial Photosynthesis, Advanced Research institute for Natural Science and Technology, Osaka City University, 3-3-138 Sugimoto, Sumiyoshi, Osaka 558-8585, Japan*

* Corresponding authors.

School of Engineering, Tohoku University,

6-6-07, Aoba, Aramaki, Aoba-ku, Sendai 980-8579, Japan

E-mail: yoshinao@erec.che.tohoku.ac.jp, Tel/Fax: +81-22-795-7215 (Y. N.);

tomi@erec.che.tohoku.ac.jp, Tel/Fax: +81-22-795-7214 (K. T.)

Table S1 Summary of reports on hydrodeoxygenation of erythritol, 1,4-anhydroerythritol, xylitol and sorbitol over heterogeneous catalysts

Entry (entry in Scheme 1)	Substrate	Catalyst	Composition	Additive/solvent	Conditions			Conv. / %	Mono-alcohol/diol (yield (%))	Ref.
					T / K	*P*(H_2) / MPa	*t* / h			
1 (a)	Erythritol	ReO_x-Pd/CeO_2	2 wt% Re, 0.3 wt% Pd	None/1,4-dioxane	433	8	24	98	1,2-BuD (79), 1,4-BuD (12)	S1
2 (b)	Erythritol	Cu/C	67 wt%	None/water	453	1.8	240	35	1,2-BuD (16)	S2
3 (b)	Erythritol	Cu/CaO-Al_2O_3	43 wt% Cu	None/water	503	2.8	10	85	1,2-BuD (39)	S3
4	Erythritol	Rh-ReO_x/ZrO_2	3.7 wt% Rh, 3.5 wt% Re	None/water	473	12	8	80	Diols mixture (29)	S4,5
5 (c)	Erythritol	Ir-ReO_x/SiO_2	4 wt% Ir, 3.9 wt% Re	H_2SO_4/water	373	8	24	74	1,4-BuD (24), 1,3-BuD (9)	S6
6 (c)	Erythritol	Ir-ReO_x/TiO_2	4 wt% Ir, 1.0 wt% Re	None/water	373	8	12	62	1,4-BuD (23)	S7
7 (d)	Erythritol	Ir-ReO_x/SiO_2	4 wt% Ir, 3.9 wt% Re	None/water	373	8	48	97	1-BuOH (34)	S7
8 (e)	1,4-Anhydro-erythritol	Rh-MoO_x/SiO_2	4 wt% Rh, 0.5 wt% Mo	None/water	393	8	48	100	2-BuOH (51)	S8
9 (f)	1,4-Anhydro-erythritol	Pt-WO_x/SiO_2	4 wt% Pt, 0.9 wt% W	None/water	413	8	80	100	1,3-BuD (54)	S9
10 (g)	1,4-Anhydro-erythritol	ReO_x-Au/CeO_2 + ReO_x/C	1 wt% Re, 0.3 wt% Au; 3 wt% Re	None/1,4-dioxane	413	8	24	100	1,4-BuD (86)	S10
11 (g)	1,4-Anhydro-erythritol	ReO_x/CeO_2 + ReO_x/C	1 wt% Re; 3 wt% Re	None/1,4-dioxane	413	8	24	97	1,4-BuD (83)	S11
12	1,4-Anhydro-erythritol	ReO_x-Au/CeO_2 + ReO_x/ WO_3-ZrO_2	1 wt% Re; 1 wt% Re	None/1,4-dioxane	413	8	24	100	1,4-BuD (53)	S12
13	Erythritol	Pt-WO_x/SiO_2	4 wt% Pt, 0.9 wt% W	None/water	413	8	50	99	1,4-BuD (51), 1,3-BuD (15)	This work
14	Erythritol	Pt-WO_x/SiO_2	4 wt% Pt, 0.9 wt% W	None/water	453	8	50	99	1-BuOH (56), 2-BuOH (17)	This work
15 (h)	Xylitol	Ir-ReO_x/SiO_2	4 wt% Ir, 3.9 wt% Re	HZSM-5, *n*-dodecane/ water	413	8	24	100	1-PeOH (18), 2- + 3-PeOHs (19)	S13

16 (i)	Xylitol	ReO_x-Pd/CeO_2	2 wt% Re, 0.3 wt% Pd	None/1,4-dioxane	433	8	24	100	1-PeOH (83), 3-PeOH (16)	S1
17	Xylitol	Pt-WO_x/SiO_2	4 wt% Pt, 0.9 wt% W	None/water	453	7	48	100	1-PeOH (30), 2-PeOH (9), 3-PeOH (20)	This work
18 (j)	Sorbitol	Ir-ReO_x/SiO_2	4 wt% Ir, 3.9 wt% Re	*n*-Dodecane/ water	413	8	75	100	3-HxOH (36), 2-HxOH (8), 1-HxOH (<1)	S14
19 (k)	Sorbitol	ReO_x-Pd/CeO_2	2 wt% Re, 0.3 wt% Pd	None/1,4-dioxane	433	8	72	100	1,2-HxD (36), 1,4-HxD (32), 3,4-HxD (11), 1,6-HxD (6)	S1
20 (l)	Sorbitol	Pt-ReO_x/Zr-P	4 wt% Pt, 3.8 wt% Re	None/water	453	6.2	Flow	-	1-HxOH (5.0) 2-HxOH (5.3) 3-HxOH (5.6) Total C4-C6 monoalcohols (28)	S15
21	Sorbitol	Ru-$Mo(acac)_2$/ CMK-3	2 wt% Ru, 2 wt% Mo	None/water	523	4	Flow	>99.9	HxOHs (7), 1,6-HxD (17)	S16
22	Sorbitol	Pt-WO_x/SiO_2	4 wt% Pt, 0.9 wt% W	None/water	453	8	72	100	3-HxOH (36), 2-HxOH (12), 1-HxOH (12)	This work

Table S2 Summary of reports on anhydroxylitol from xylitol or xylose

Substrate	Catalyst	Composition	Heterogeneous system?	Additive/ solvent	Conditions			Anhydro-xylitol (yield (%))	Ref.
					T / K	$P(H_2)$ / MPa	*t* / h		
Xylitol	None	-	No	None/ water	548	Air	12	~90	S17
Xylitol	$H_4SiW_{12}O_{40}$	-	No	None/ water	453-473	5	n.d.	1,4- (n.d.)	S18
Xylitol	H_2SO_4	-	No	None/ dioxane-water	453, micro wave	Air	0.25	1,4- (85), 2,5- (13)	S19
Xylose	Ru@Dowex-H	0.2 wt% Ru	Yes	None/ water	463	3	6	(95)	S20
Xylitol	WO_x/SiO_2	0.94 wt% W	Yes	None/ water	453	1	240	1,4- (94)	This work

n.d.: no data.

Note on the stereochemistry of 1,4-anhydroxylitol:

There are one set of enantiomers of 1,4-anhydroxylitol: (2*R*, 3*R*, 4*S*)-2-(hydroxymethyl)tetrahydrofuran-3,4-diol and (2*S*, 3*S*, 4*R*)-2-(hydroxymethyl)tetrahydrofuran-3,4-diol. The former form corresponds to the dehydration at 1,4-positions of D-xylose, and it can be expressed by "1,4-anhydro-D-xylitol". The expression "2,5-anhydroxylitol" might represent the other enantiomer. However, because xylitol is a *meso* compound, the racemic mixture of 1,4-anhydroxylitol should be produced by chemical dehydration of xylitol, while biological production methods may give a pure enantiomer. Conventional analysis methods including ours cannot separate these enantiomers. The "1,4-anhydroxylitol" produced in our system was the racemic mixture, and probably so in the literature systems listed above.

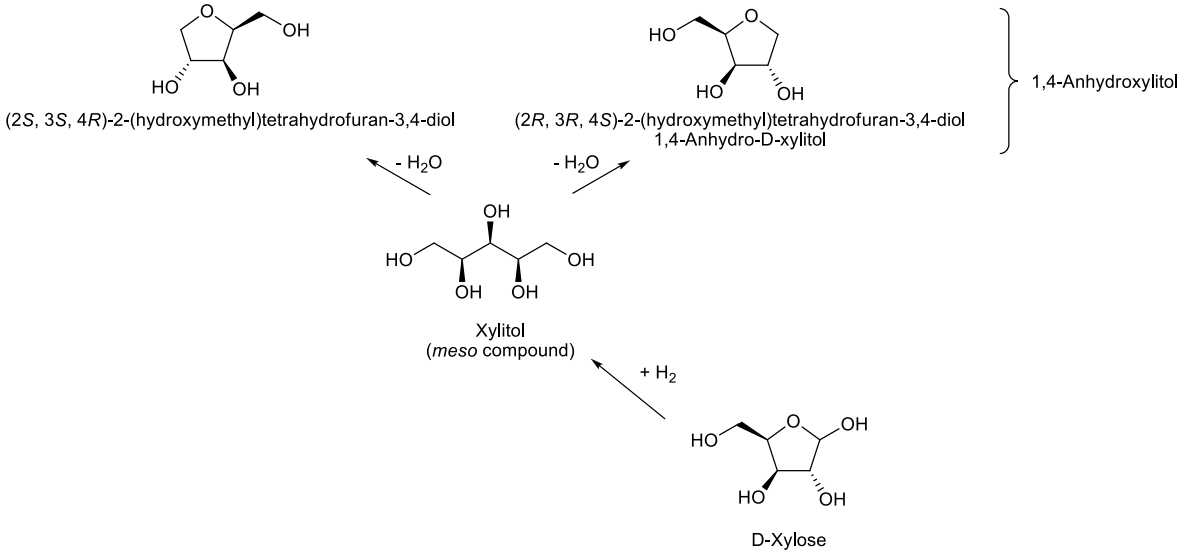

Table S3 Dehydration of xylitol over 0.94 wt% WO_x/SiO_2 catalysts

Entry	$P(H_2)$ / MPa	t / h	Conv. / %	Selectivity / %		C. B. / %	Highest yield / %
				1,4-Anhydroxylitol	Others		
1	7	144	63.6	99.5	0.5	101.3	-
2	1	144	64.2	99.5	0.5	100.3	-
3	1[a]	144	82.5	99.2	0.8	100.1	-
4	1[b]	240	96.2	96.7	3.3	101.2	94.1[c]

Reaction conditions: W_{cat} = 0.2 g, H_2O = 4 g, xylitol = 0.5 g, T = 453 K, stirring rate = 250 rpm.

a: W_{cat} = 0.8 g, H_2O = 5 g, xylitol = 2.0 g, T = 453 K, stirring rate = 500 rpm.

b: W_{cat} = 1.0 g, H_2O = 5 g, xylitol = 2.0 g, T = 453 K, stirring rate = 500 rpm.

c: About 10% of isomers of 1,4-anhydroxylitol was contained as identified by GC-MS (Figure S4).

Table S4 Hydrogenolysis of 1,4-anhydro-xylitol over Pt-WO_x/SiO_2 (4 wt% Pt, W/Pt = 0.25) at lower temperature (413 K)

t / h	Conv. / %	Selectivity / %												C. B. / %
		1-PeOH	3-PeOH	2-PeOH	1,5-PeD	1,4-/1,3-/2,3-PeD	1,2-PeD	1,2,5-PeT	Other triols (1,3,5-PeT, main)	1,2,3,5-Pentane-tetraol (main)	Alkanes	2-MTHF	Others	
4	82.2	0.9	0.3	0	4.0	2.7	0	4.9	19.3	66.8	1.1	0	0	90.2
16	98.9	2.0	0.4	0.4	8.0	8.9	0	4.7	40.6	33.5	1.6	0	0	90.0
24	99.8	2.1	0.4	0.4	8.5	9.9	0	4.7	40.5	32.1	1.4	0	0	95.5
48	100	3.0	0.5	0.5	9.3	14.2	0	5.2	48.9	16.4	2.1	0	0	96.9
48[a]	100	8.1	1.5	1.1	13.5	27.6	0	1.8	43.6	2.3	0.7	0.4	0	93.6
72	100	7.7	1.7	1.4	12.5	29.2	0	1.5	41.2	1.5	2.5	0.7	0	90.9

Reaction conditions: W_{cat} = 0.2 g, H_2O = 4 g, 1,4-anhydro-xylitol = 0.25 g, T = 413 K, $P(H_2)$ = 7 MPa.

a: xylitol = 0.25 g.

PeOH = pentanol, PeD = pentanediol, PeT = pentanetriol, MTHF = methyltetrahydrofuran.

Table S5 Comparison of hydrogenolysis of related alcohols over non-reduced and reduced Pt-WO_x/SiO_2 (4 wt% Pt, W/Pt = 0.25) catalyst

Substrate	Pre-reduction method	*t* / h	Conv. / %	Products (Selectivity / %)	C. B. / %
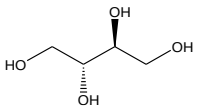	(L, 473)	50	99.3	1,4-BuD (54.1), 1,2,4-BuT (4.6), 1,3-BuD (15.9), 1,2,3-BuT (5.0), 1-BuOH (14.3), 2-BuOH (5.0), 2,3-BuD (0.8), Others (0.3)	95.7
	Non-pre-reduced	25	100	1,4-BuD (40.2), 1,2,4-BuT (0.8), 1,3-BuD (13.7), 1,2,3-BuT (11.8), 1-BuOH (26.6), 2-BuOH (5.7), Others (1.2)	94.5

Reaction conditions: W_{cat} = 0.2 g, erythritol = 0.5 g, $P(H_2)$ = 8 MPa, T = 413 K.

BuT = butanetriol, BuD = butanediol, BuOH = butanol.

Table S6 Time course of the erythritol hydrodeoxygenation over Pt-WO_x/SiO_2 (4 wt% Pt, W/Pt = 0.25) catalyst at lower temperature (413 K)

t / h	Conv. / %	Selectivity / %									C. B. / %
		1,4-BuD	1,2,4-BuT	1,3-BuD	1,2,3-BuT	1-BuOH	2-BuOH	1,2-BuD	2,3-BuD	Others	
0	2.4	-	-	-	-	-	-	-	-	-	93.2
2	22.5	7.7	64.3	6.1	16.8	2.0	2.6	0.5	0	0	90.9
6	35.8	14.9	56.1	7.2	15.6	2.3	2.7	1.2	0	0	93.8
12	54.3	21.9	43.8	9.9	16.8	2.7	2.5	1.2	0.4	0.8	96.0
24	82.5	40.3	23.8	12.6	12.2	6.0	3.5	1.0	0.6	0	93.7
42	95.0	49.0	15.7	13.2	9.1	7.5	3.8	0	0.7	1.2	95.2
50	99.3	54.1	4.6	15.9	5.0	14.3	5.0	0	0.8	0.3	95.7
60	100	52.4	3.3	16.2	4.1	17	5.7	0	0.8	0.5	91.7

Reaction conditions: Erythritol = 0.5 g, H_2O = 4 g, W_{cat} = 0.2 g, $P(H_2)$ = 8 MPa, T = 413 K. Reduction conditions: (L, 473). BuT = butanetriol, BuD = butanediol, BuOH = butanol.

Table S7 Curve fitting results of Pt L_2-edge EXAFS of Pt-WO_x/SiO_2 (4 wt% Pt, W/Pt = 0.25) after reaction

Entry	Catalyst	Shells	CN[b]	R / 10^{-1} nm[c]	σ / 10^{-1} nm[d]	ΔE_0 / eV[e]	R_f / %[f]	FF range / nm[g]
1[a]	Pt-WO_x/SiO_2 (calcined)	Pt-Pt (or -W) Pt-O	3.1 2.4	2.75 2.04	0.062 0.060	-1.4 -1.7	1.3	0.117-0.310
2[a]	Pt-WO_x/SiO_2 (413 K)	Pt-Pt (or -W)	10.1	2.76	0.072	-1.5	0.2	0.166-0.328
3	Pt-WO_x/SiO_2 (453 K)	Pt-Pt (or -W)	10.0	2.75	0.071	-0.4	0.3	0.166-0.328
4	Pt foil	Pt-Pt	12	2.77	0.060	0.0	-	-
5	$Na_2Pt(OH)_6$	Pt-O	6	2.05	0.060	0.0	-	-

[a]Ref. S21. [b]Coordination number. [c]Bond distance. [d]Debye-Waller factor. [e]Difference in the origin of photoelectron energy between the reference and the sample. [f]Residual factor. [g]Fourier filtering range.

The spectra of Pt L_2-edge EXAFS were shown in Figure S11.

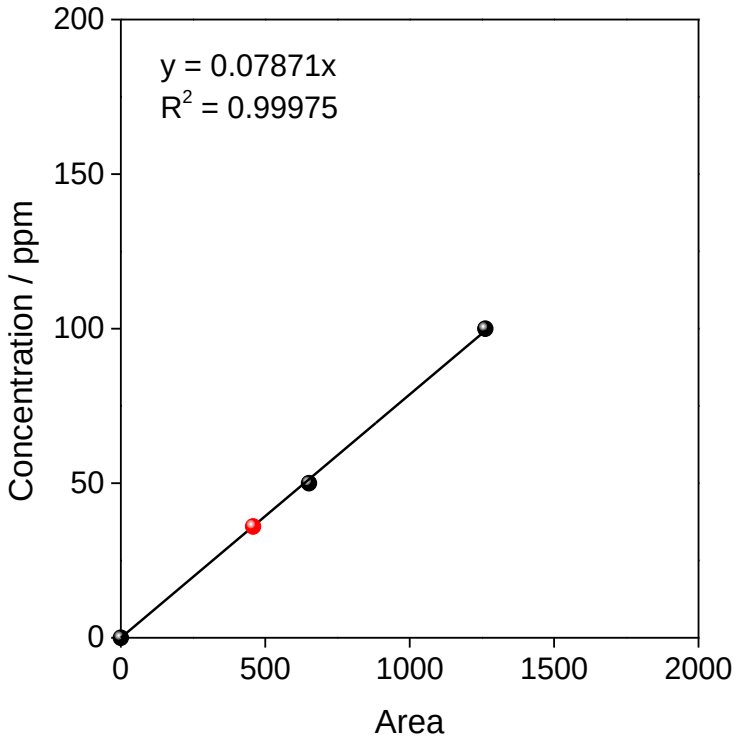

Figure S1. Calibration curve for TOC measurement (red dot, reaction sample; black dot, standard samples)
Reaction conditions: W_{cat} = 0.2 g, H_2O = 4 g, xylitol = 0.5 g, T = 453 K, t = 48 h, $P(H_2)$ = 5 MPa.

Details for calculation:

Mole of carbon in the xylitol: 0.5062/152.15×5×1000 = 16.63 mmol

Mole of carbon in the gas phase: 0.45 mmol

Mole of carbon in the liquid phase (on the basis of potassium hydrogen phthalate (standard materials)): 36 (ppm)×0.1(L)/1000/(0.5062/(0.5062 + 4.0047 (amount of H_2O solvent) + 49.9182 (amount of H_2O for recovery)))×/204.22×8×1000 = 15.16 mmol

Carbon balance: (15.16 + 0.45)/16.63×100 = 93.9%

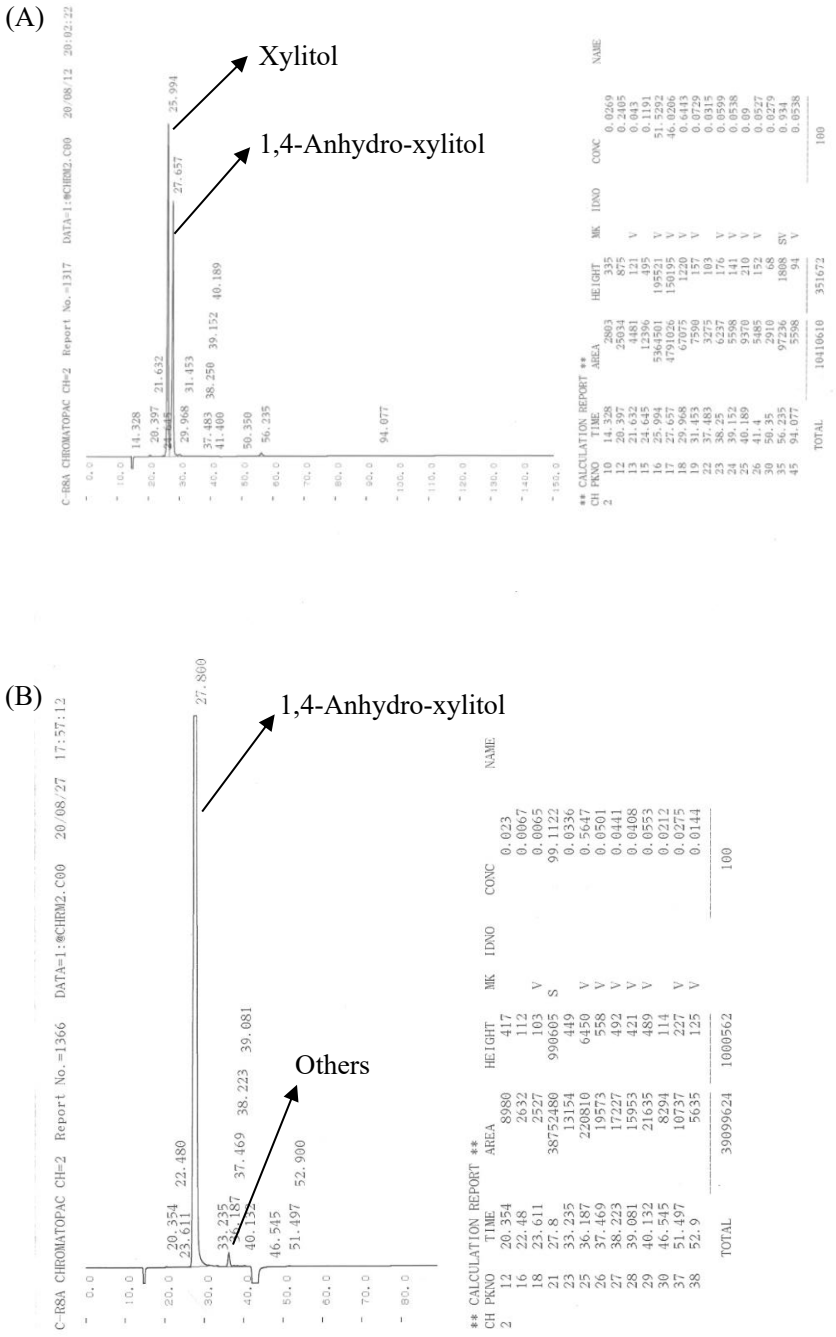

Figure S2. Original data of HPLC for (A) dehydration of xylitol over 0.94 wt% WO_x/SiO_2 (453 K, 48 h, the internal standard was not added), and (B) the same sample after purification by column chromatography.

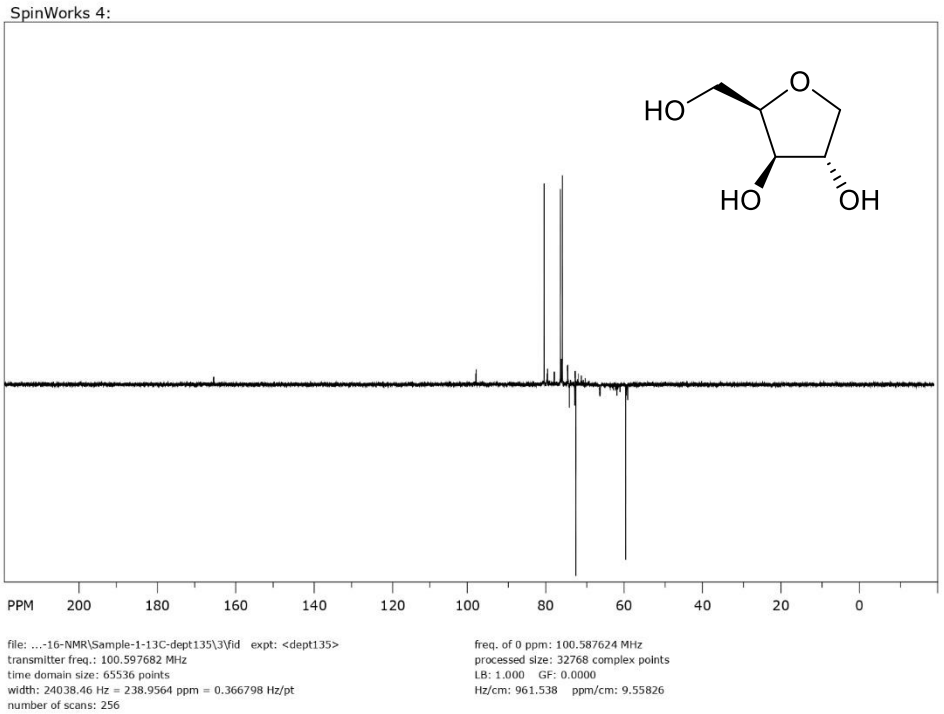

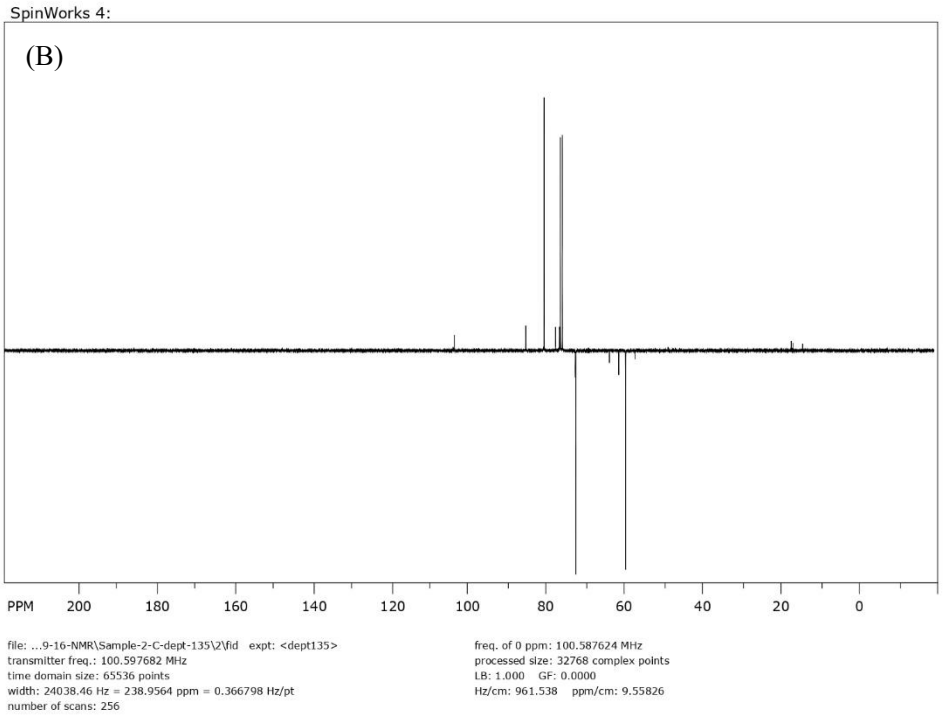

Figure S3. ^{13}C NMR DEPT 135 spectra of (A) commercial 1,4-anhydro-D-xylitol (TCI), and (B) as synthesized by xylitol dehydration over WO_x/SiO_2. Note: this analysis cannot determine the distribution of enantiomers. The synthesized products were racemic mixture.

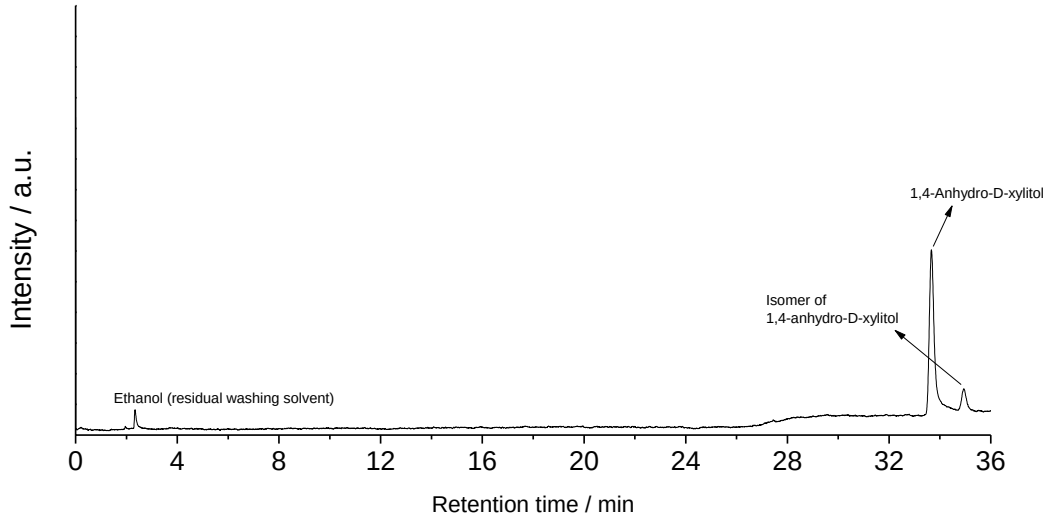

Figure S4. GC chart of the synthesized 1,4-anhydroxylitol by xylitol dehydration over WO_x/SiO_2.

Notes:

Small amount of ethanol (washing solvent) cannot be separated. The purity of 1,4-anhydroxylitol was about 90% on the basis of GC chart area. Reaction conditions: W_{cat} = 1.0 g, H_2O = 5 g, xylitol = 2.0 g, t = 240 h, $P(H_2)$ = 1 MPa, T = 453 K, stirring rate = 500 rpm (Table S3, entry 4).

The peak of "1,4-Anhydro-D-xylitol" means the same peak position of commercial 1,4-anhydro-D-xylitol. The actual product was the racemic mixture.

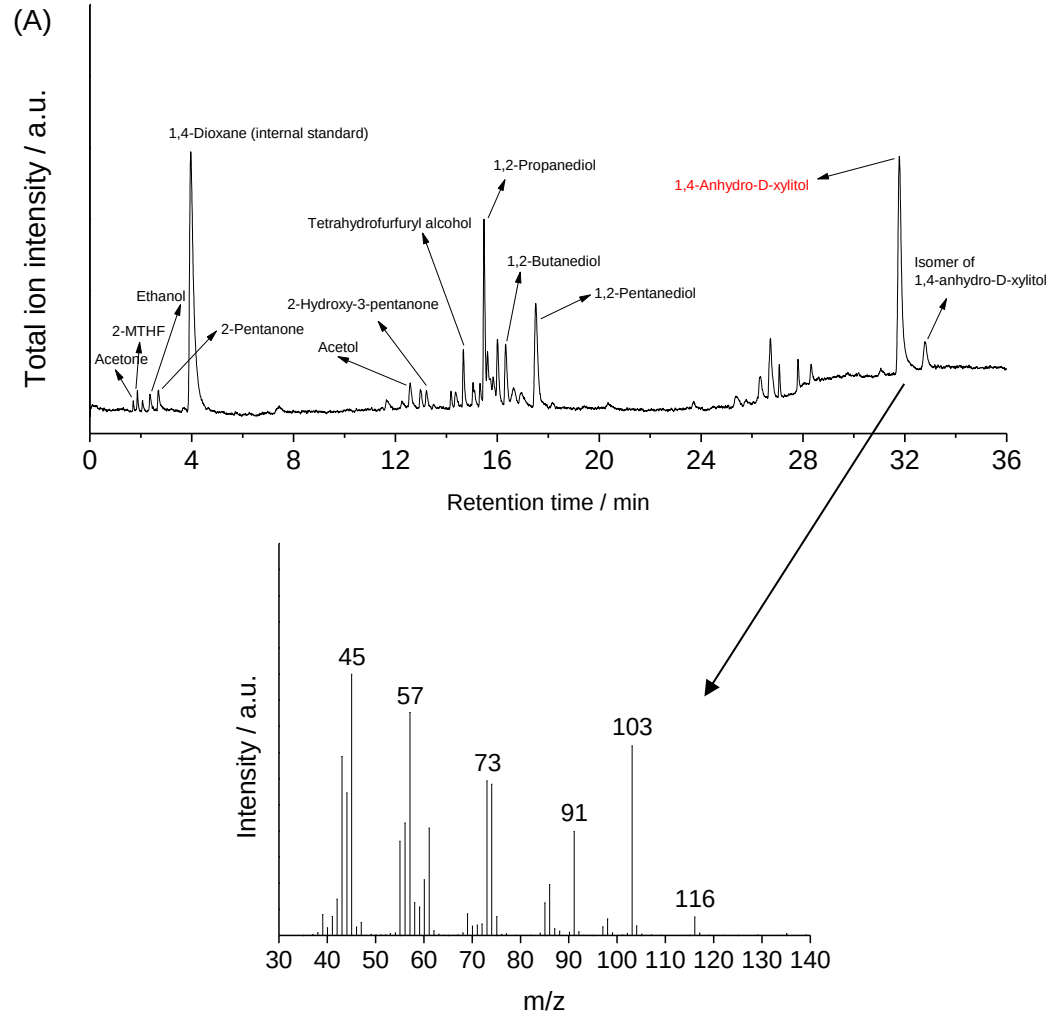
(A)
Total ion intensity / a.u.
1,4-Dioxane (internal standard)
1,2-Propanediol
1,4-Anhydro-D-xylitol
Tetrahydrofurfuryl alcohol
1,2-Butanediol
Isomer of
1,4-anhydro-D-xylitol
Ethanol
1,2-Pentanediol
2-Hydroxy-3-pentanone
2-MTHF
2-Pentanone
Acetone
Acetol
0 4 8 12 16 20 24 28 32 36
Retention time / min
Intensity / a.u.
45
57
73
91
103
116
30 40 50 60 70 80 90 100 110 120 130 140
m/z

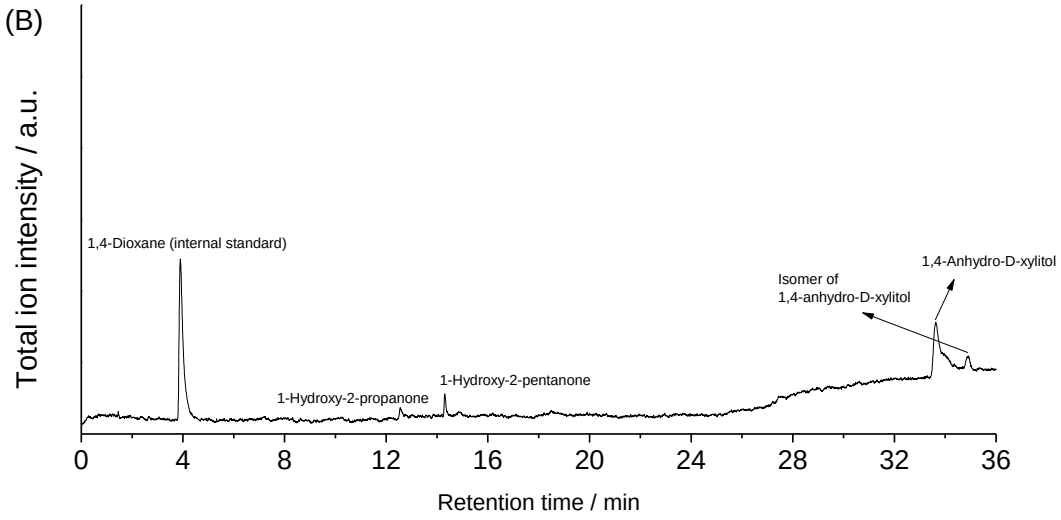
(B)
Total ion intensity / a.u.
1,4-Dioxane (internal standard)
1,4-Anhydro-D-xylitol
Isomer of
1,4-anhydro-D-xylitol
1-Hydroxy-2-pentanone
1-Hydroxy-2-propanone
0 4 8 12 16 20 24 28 32 36
Retention time / min

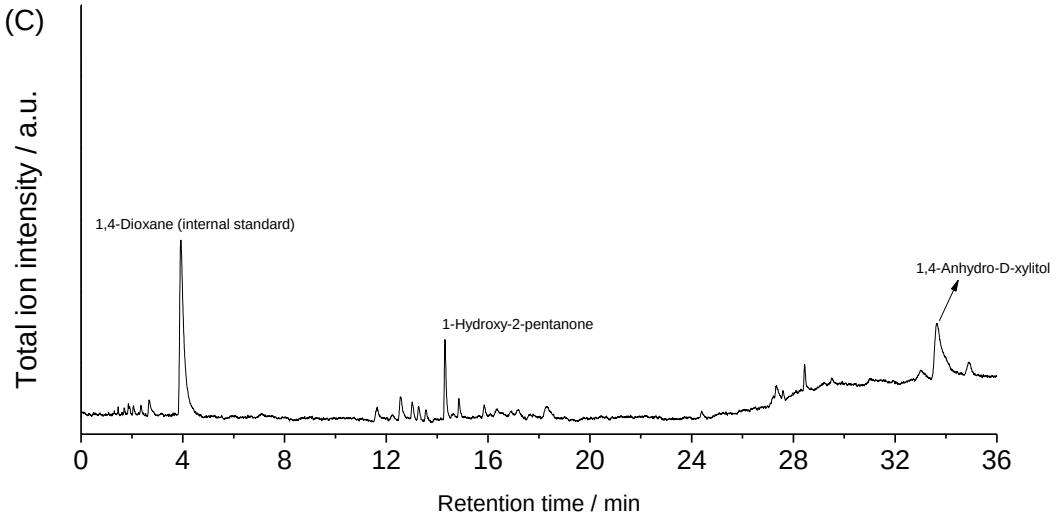

Figure S5. GC-MS results of (A) xylitol conversion over Pt-WO_x/SiO_2 under Ar for 48 h and MS spectra for the main peak, (B) xylitol conversion over Pt-WO_x/SiO_2 under Ar for 4 h, and (C) xylitol conversion over the pre-reduced Pt-WO_x/SiO_2 catalyst under Ar for 4 h.

Notes:

The unconverted xylitol cannot be detected by GC.

The peak of "1,4-Anhydro-D-xylitol" means the same peak position of commercial 1,4-anhydro-D-xylitol. The actual product was the racemic mixture.

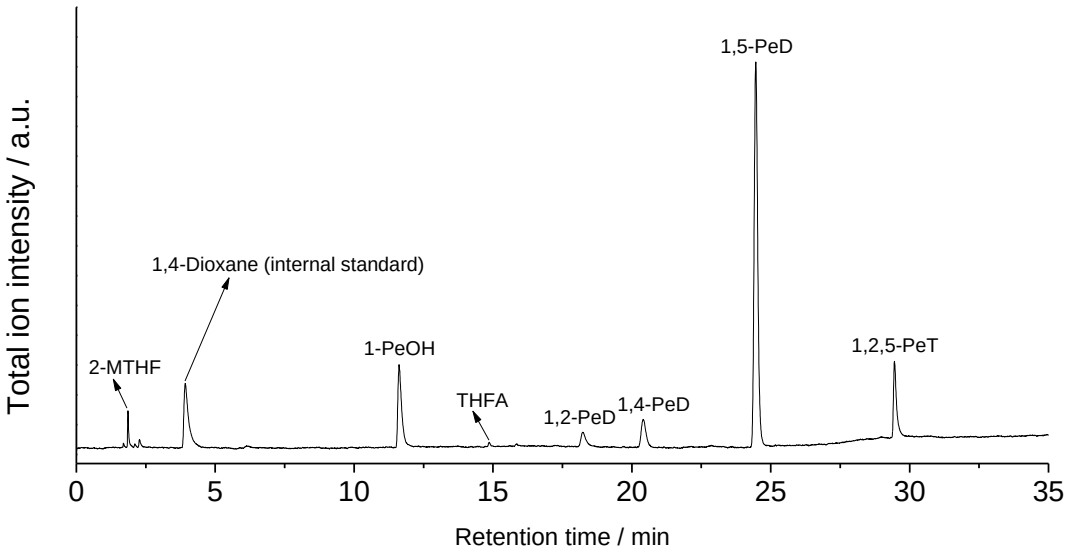

Figure S6. GC-MS results of 1,2,5-PeT hydrodeoxygenation at 453 K for 4 h. (Table 3, entry 5, the mass spectra not shown).

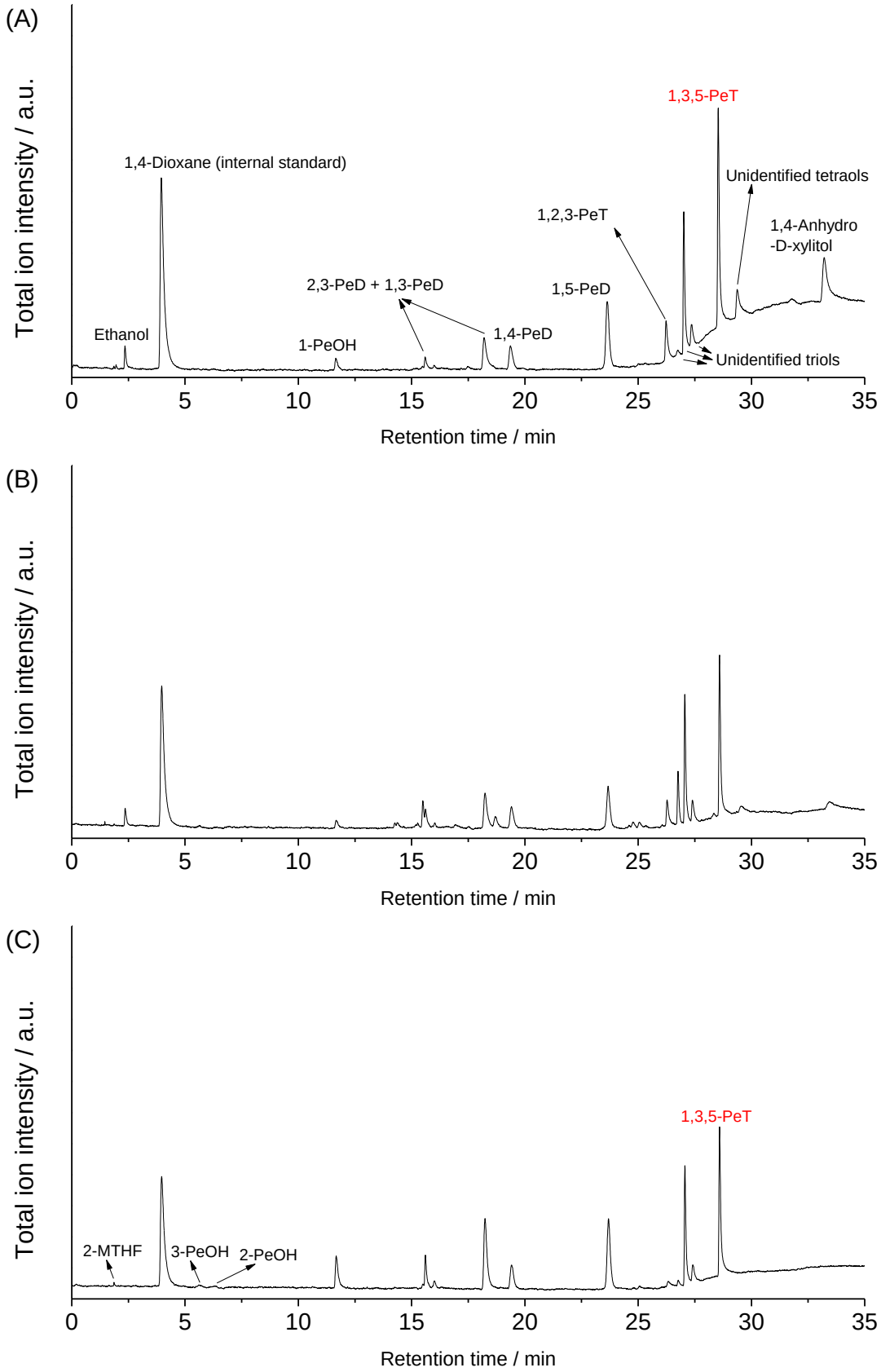

Figure S7. GC-MS results of 1,4-anhydro-D-xylitol hydrogenolysis for (A) 16 h, (B) 48 h, and (C) xylitol hydrogenolysis for 48 h at 413 K (Table S4, the mass spectra not shown).

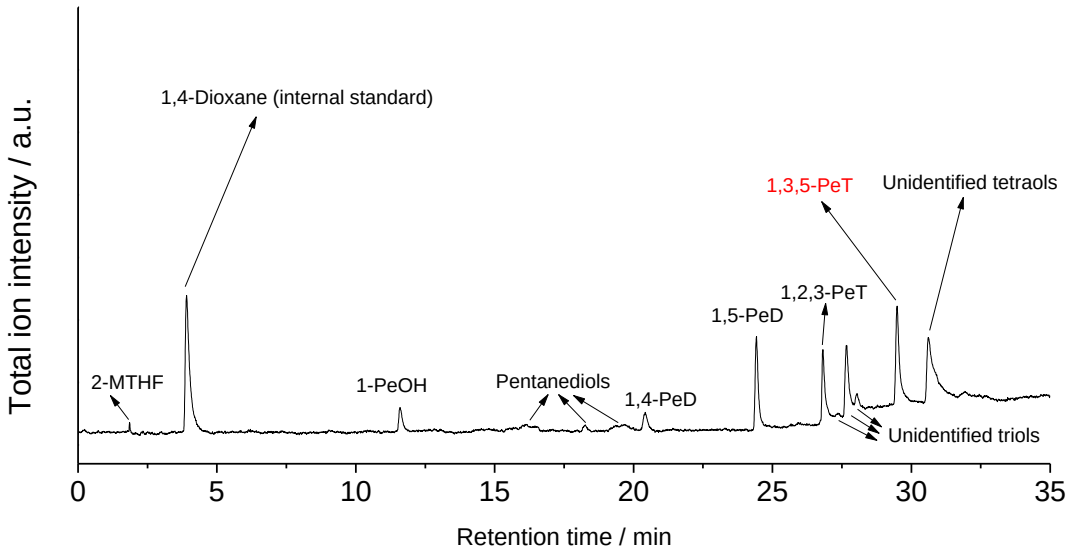

Figure S8. GC-MS results of xylitol hydrodeoxygenation at 453 K for 4 h. (Table 3, entry 10, the mass spectra not shown).

Note: The unconverted xylitol cannot be detected by GC, and no detectable 1,4-anhydroxylitol was confirmed.

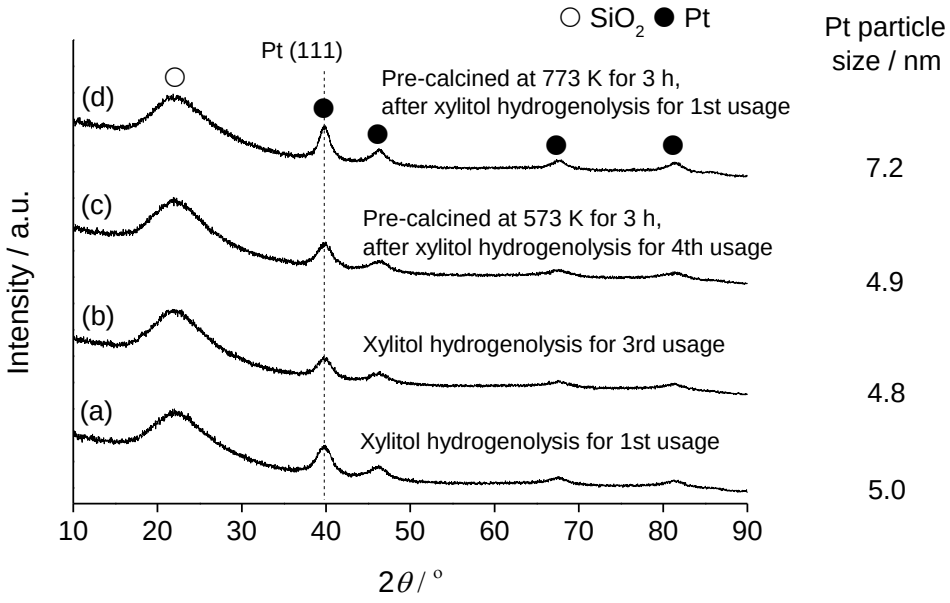

Figure S9. XRD patterns of the Pt-WO_x/SiO_2 (4 wt% Pt, W/Pt = 0.25) catalyst after catalytic use. No calcination was performed for (a) and (b), (c) pre-calcined at 573 K for 3 h before each reuse test, and (d) pre-calcined at 773 K for 3 h before reuse test. The Pt particle size was calculated by the width of Pt (111) peak and Scherrer's equation.

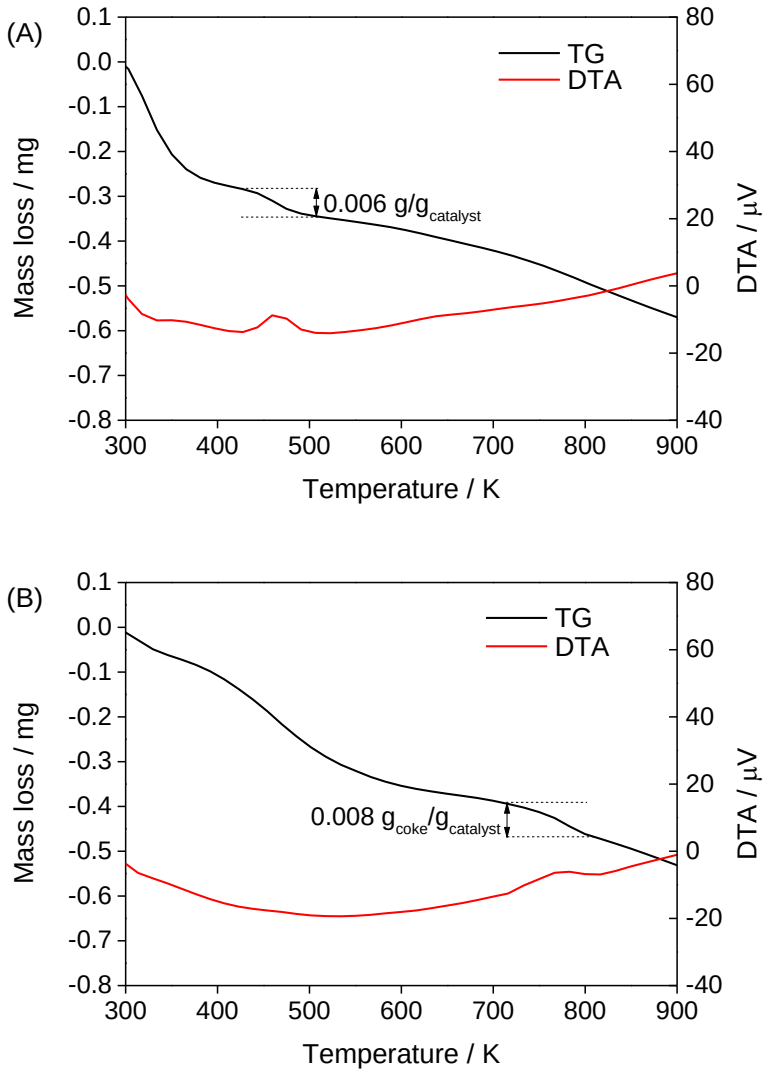

Figure S10. TG-DTA profiles of Pt-WO_x/SiO_2 catalyst after reaction. Measurement conditions: sample weight of about 10 mg, heating rate 10 K/min under air. Reaction conditions: $P(H_2)$ = 7 MPa, T = 453 K, t = 48 h, xylitol = 0.5 g, H_2O: 4 g, W_{cat} = 0.2 g, (A) after first usage (Table 4, entry 1) and (B) after 3 times usage without any calcination during recovery (Table 4, entry 3).

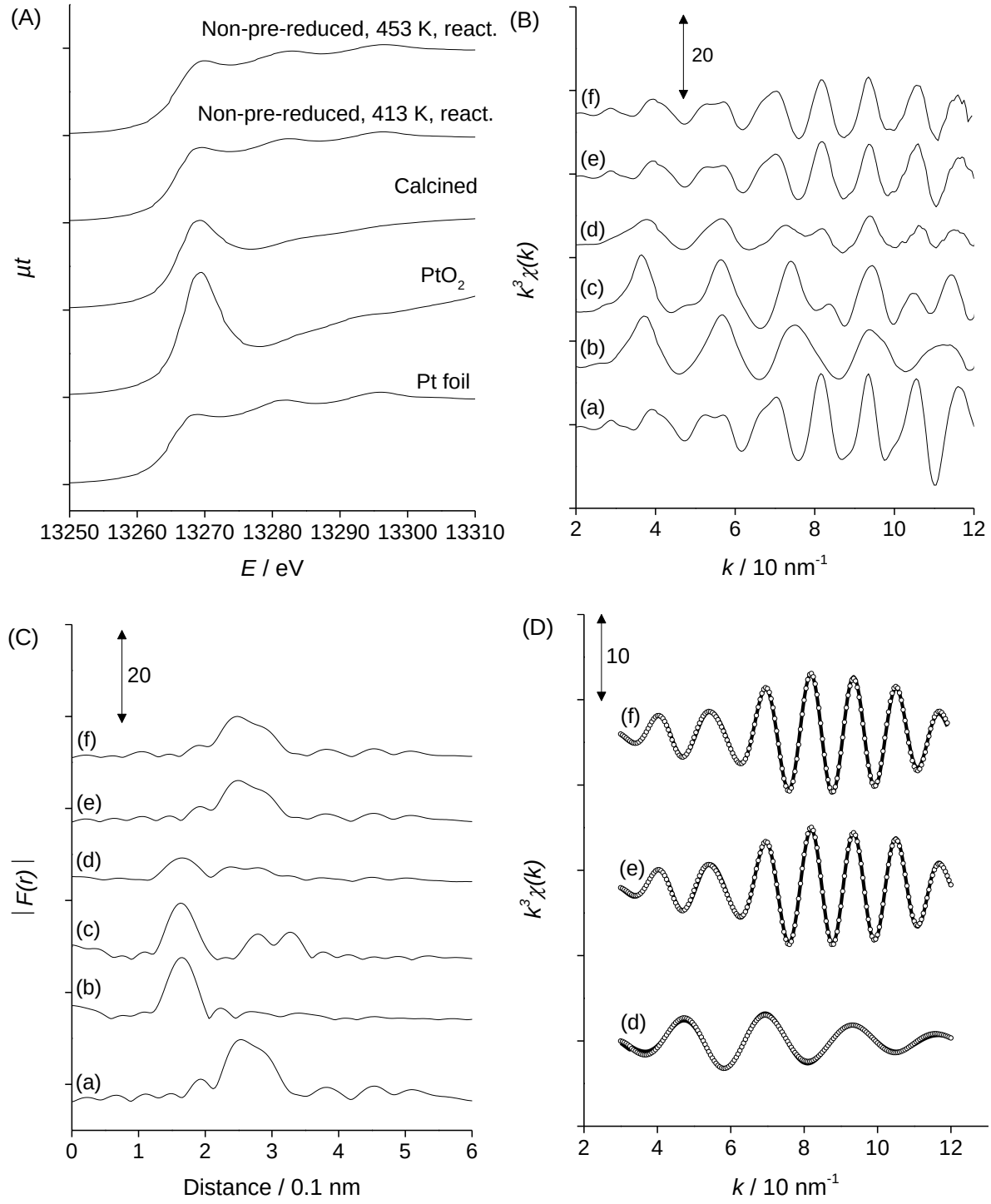

Figure S11. Results of Pt L_2-edge (A) XANES and (B~D) EXAFS analysis of Pt-WO_x/SiO_2 (4 wt% Pt, W/Pt = 0.25) catalysts after reaction catalysts after reaction. (A) k^3-Weighted EXAFS oscillations. (B) Fourier transform of k^3-weighted Pt L_2-edge EXAFS, FT range: 30-120 nm^{-1}. (C) Fourier transform of k^3-weighted Pt L_2-edge EXAFS, FT range: 30-120 nm^{-1}. (D) Fourier filtered EXAFS data (solid line) and calculated data (dotted line). (a) Pt foil, (b) $Na_2Pt(OH)_6$, (c) PtO_2, (d) Pt-WO_x/SiO_2 (4 wt% Pt, W/Pt = 0.25) after calcination, (e) Pt-WO_x/SiO_2 after reaction (413 K), data from ref. S21, (f) Pt-WO_x/SiO_2 after reaction (453 K). The curve fitting result is listed in Table S7.

References

S1. N. Ota, M. Tamura, Y. Nakagawa, K. Okumura and K. Tomishige, *Angew. Chem. Int. Ed.*, 2015, **54**, 1897-1900.

S2. W. Wang, K. Nakagawa, T. Yoshikawa, T. Masuda, E. Fumoto, Y. Koyama, T. Tago and H. Fujitsuka, *Appl. Catal. A*, 2021, **619**, 118152.

S3. X. Jin, J. Shen, W. Yan, M. Zhao, P. S. Thapa, B. Subramaniam and R. V. Chaudhari, *ACS Catal.*, 2015, **5**, 6545-6558.

S4. A. Said, D. Da Silva Perez, N. Perret, C. Pinel and M. Besson, *ChemCatChem*, 2017, **9**, 2768-2783.

S5. A. Sadier, N. Perret, D. Da Silva Perez, M. Besson and C. Pinel, *Appl. Catal. A*, 2019, **586**, 117213.

S6. Y. Amada, H. Watanabe, Y. Hirai, Y. Kajikawa, Y. Nakagawa and K. Tomishige, *ChemSuschem*, 2012, **5**, 1991-1999.

S7. M. Gu, L. Liu, Y. Nakagawa, C. Li, M. Tamura, Z. Shen, X. Zhou, Y. Zhang and K. Tomishige, *ChemSusChem*, 2021, **14**, 642-654.

S8. T. Arai, M. Tamura, Y. Nakagawa and K. Tomishige, *ChemSuschem*, 2016, **9**, 1680-1688.

S9. L. Liu, T. Asano, Y. Nakagawa, M. Tamura and K. Tomishige, *Green Chem.*, 2020, **22**, 2375-2380.

S10. T. M. Wang, S. B. Liu, M. Tamura, Y. Nakagawa, N. Hiyoshi and K. Tomishige, *Green Chem.*, 2018, **20**, 2547-2557.

S11. T. Wang, M. Tamura, Y. Nakagawa and K. Tomishige, *ChemSusChem*, 2019, **12**, 3615-3626.

S12. T. Wang, Y. Nakagawa, M. Tamura, K. Okumura and K. Tomishige, *React. Chem. Eng.*, 2020, **5**, 1237-1250.

S13. K. Y. Chen, M. Tamura, Z. L. Yuan, Y. Nakagawa and K. Tomishige, *ChemSuschem*, 2013, **6**, 613-621.

S14. S. B. Liu, Y. Okuyama, M. Tamura, Y. Nakagawa, A. Imai and K. Tomishige, *ChemSusChem*, 2015, **8**, 628-635.

S15. J. Lee, I. Ro, H. J. Kim, Y. T. Kim, E. E. Kwon and G. W. Huber, *Process Safety Environ. Protection*, 2018, **115**, 2-7.

S16. Y. Yu, Q. Zhang, X. Chen, Y. Liu, Y. Qin, S. Qiu, H. Li and T. Wang, *Fuel Process. Technol.*, 2020, **197**, 106195.

S17. A. Yamaguchi, N. Muramatsu, N. Mimura, M. Shirai and O. Sato, *Phys. Chem. Chem. Phys.*, 2017, **19**, 2714-2722.

S18. J. U. Oltmanns, S. Palkovits and R. Palkovits, *Appl. Catal. A*, 2013, **456**, 168-173.

S19. J. M. Robinson, A. M. Wadle, M. D. Reno, R. Kidd, S. R. Barrett Hinsz and J. Urquieta, *Energy Fuels*, 2015, **29**, 6529-6535.

S20. P. Barbaro, F. Liguori and C. Moreno-Marrodan, *Green Chem.*, 2016, **18**, 2935-2940.

S21. L. Liu, T. Asano, Y. Nakagawa, M. Gu, C. Li, M. Tamura and K. Tomishige, *Appl. Catal. B*, 2021, **292**, 120164.